Ediacaran Reef Construction and the Earliest Evidence for Animal Biomineralization

Ashely Fernandes | GEOL394 | Spring 2020 | Advisor: Dr. Alan Jay Kaufman

UNIVERSITY OF MARYLAND 1856
DEPARTMENT OF GEOLOGY

Introduction & Background

The earliest evidence of animals capable of biomineralizing shells, *Cloudina*, was recently discovered in Ediacaran-aged strata of the lower Nama Group in Arasab farmstead, Namibia. The specimens are preserved in close association with microbial mats. The appearance of the *Cloudina* coincides with the end of the greatest carbon isotope anomaly in Earth history, the Shuram Excursion, at 575 Ma (Rooney, 2019). This study analyzes (i) whether the *Cloudina* contributed to the construction of microbial reefs, (ii) the original composition of the *Cloudina* shells, (iii) if the *Cloudina* fractionated seawater isotopic compositions ($\delta^{13}C$ and $\delta^{18}O$) to form their shells, and (iv) if *Cloudina* harbored sulfide-oxidizing bacteria within their bodies in a symbiotic relationship that provided the *Cloudina* with organic food.

Hypotheses

- ❖ **Reef Construction**: *Cloudina* preserved in microbial mats reflect in-situ growth because they appear to be intact, in life-position, and interlayered with the mats.
- ❖ **Shell Composition**: *Cloudina* shells from the Arasab locality contain primary phosphate minerals because the Shuram Excursion brought about high concentrations of phosphorus in the ocean (Cui et al., 2016).
- ❖ **Vital Effects**: Early *Cloudina* did not fractionate the seawater isotopic composition because the vital effect has not previously been observed in *Cloudina* (Grant, 1992).
- ❖ **Feeding Mechanism:** *Cloudina* had chemosymbionts, in the form of sulfide-oxidizing bacteria, living within them that helped them to manage the sulfide in their surroundings because a similar process is observed in the modern-day deep-sea tube worm, *Riftia pachyptila* (Felbeck, 1981).

Methods

Figure 1: Samples. 1A: Boulders were analyzed at the micro- and macroscopic levels. **1B:** Cross sections of boulders (slabs) were analyzed with a micro-XRF spectrometer at the cm-scale. Slabs were also micro-drilled for $\delta^{13}C$ and $\delta^{18}O$ analyses. **1C:** 30-µm thin sections were analyzed with a petrographic microscope and an EPMA at the mm-scale.

- ❖ **Reef Construction**: Hand specimen, ultra-high resolution GigaPan image, & Adobe Photoshop were used to make observations and measurements
- ❖ **Shell Composition**: Electron probe micro-analyzer (EPMA) & Micro x-ray fluorescence (micro-XRF) spectrometer were used to generate elemental maps
- ❖ **Vital Effects**: Multiflow isotope ratio mass spectrometer was used to measure $\delta^{13}C$ and $\delta^{18}O$
- ❖ **Feeding Mechanism**: Multicollector isotope ratio mass spectrometer was used to measure $\delta^{34}S$

Results

❖ Reef Construction

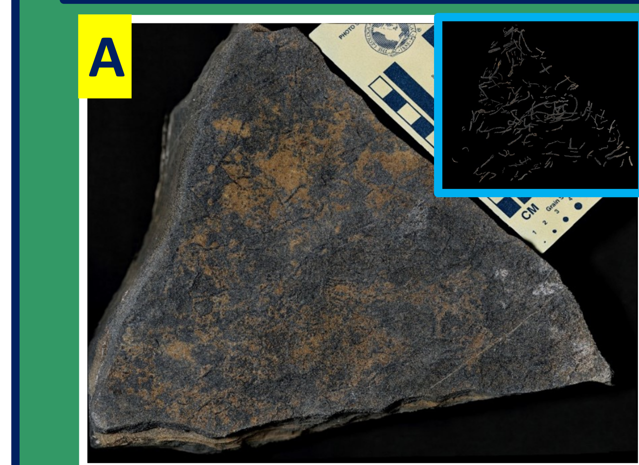

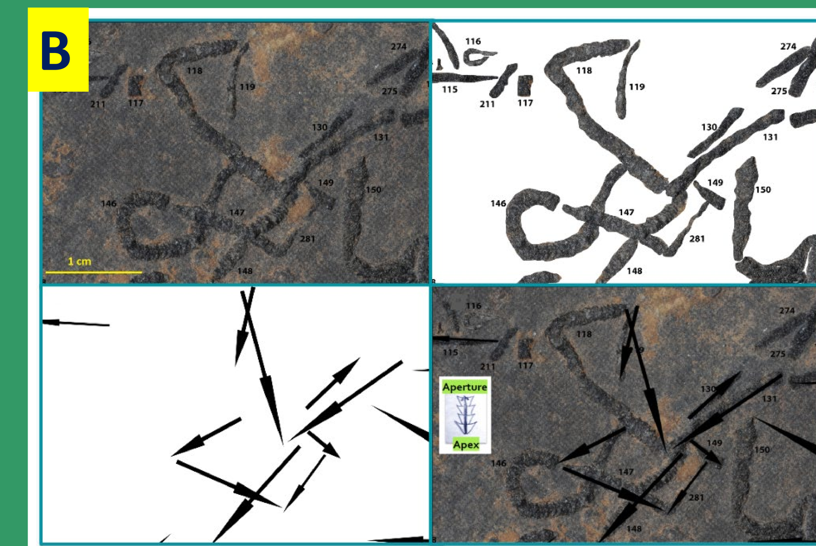

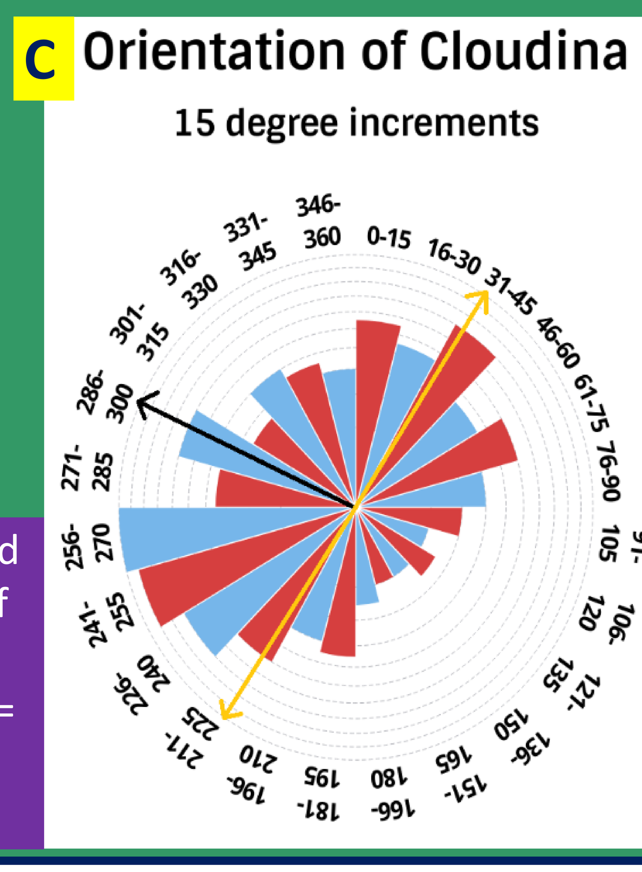

Figure 2: 2A: GigaPan image of hundreds of *Cloudina* exposed on the surface of lithified microbial mats. The inset shows 288 *Cloudina*. **2B:** Adobe Photoshop measurements of the growth direction of several *Cloudina*. **2C**: Rose diagram compiling 193 individual orientations into 15° intervals. **Black Resultant Vector:** Magnitude = 0.25, Orientation = 295°, and Circular Variance = 0.75. **Orange Resultant Vector** (accounting for bimodal variance): Magnitude = 0.27, Orientation = 33° & 213°, and Circular Variance = 0.73.

❖ Shell Composition

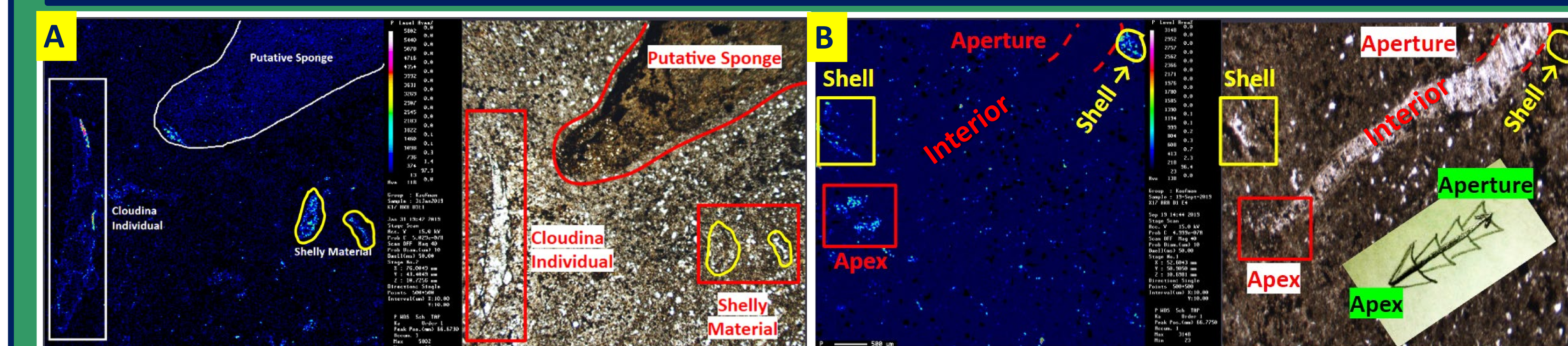

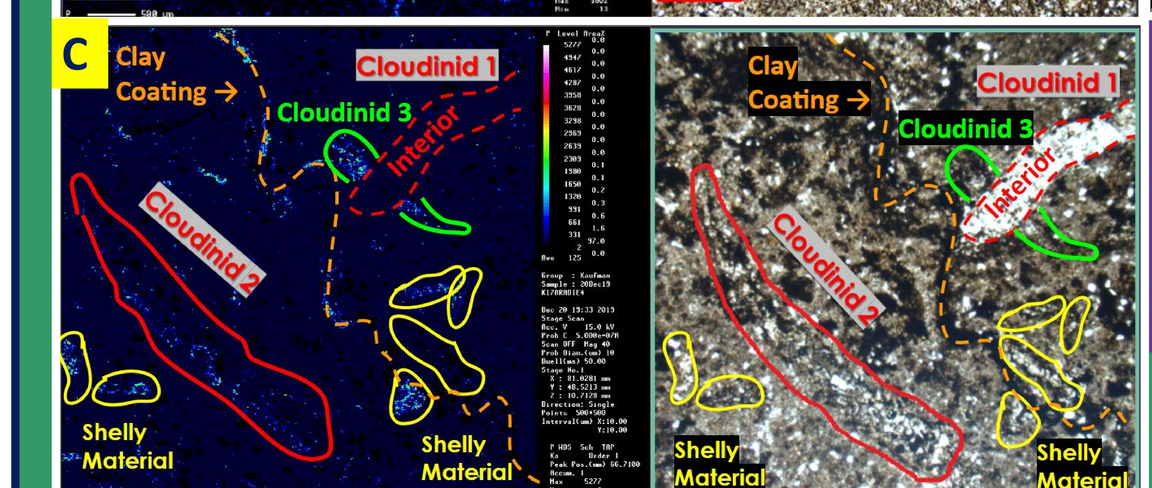

Figure 3: EPMA Data (Three Examples). Left: WDS phosphorus (P) maps. Right: Petrographic images of the areas analyzed (PPL, 1.5x). P is elevated in areas associated with *Cloudina* shells but lacking in the microbial mat and *Cloudina* interior. EDS spectra indicate the presence of apatite ($Ca_5(PO_4)_3(OH,F,Cl)$).

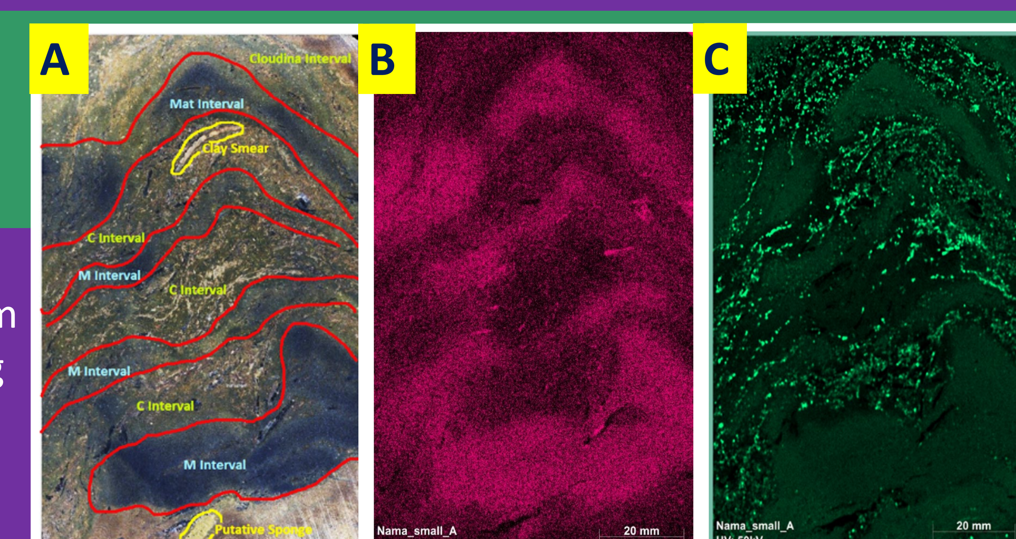

Figure 4: Micro-XRF Data. 4A: Slab consisting of alternating *Cloudina*-dominated and mat-dominated intervals. **4B:** Strontium (Sr) map showing that *Cloudina*-intervals are significantly lacking in Sr, a proxy for aragonite (Siegel, 1960). **4C:** Manganese (Mn) map showing that mat-intervals are significantly lacking in Mn clusters, signifying a change in redox conditions.

❖ Vital Effects

Comparison of the *Cloudina* and black microbial mats (a proxy for seawater conditions) reveal similar values for $\delta^{13}C$ (-4.25‰ +/- 0.46‰ and -4.36‰ +/- 0.42‰, respectively).

❖ Feeding Mechanism

Figure 5: The *Cloudina* layer on the surface of lithified microbial mats is 13.14‰ to 22.76‰ more enriched in ^{32}S than the underlying mats.

Discussion & Conclusions

❖ **Reef Construction: Hypothesis is supported**

- ❖ Based on the high circular variance and low resultant magnitude, the *Cloudina* are randomly oriented
- ❖ Detrital *Cloudina* shells would have likely become aligned and broken up by the waves that deposited them (Becker-Kerber et al. 2017), so the *Cloudina* in this study are in situ

❖ **Shell Composition: Hypothesis is supported**

- ❖ An original aragonitic shell composition can be ruled out
- ❖ *Cloudina* likely took advantage of the high availability of Ca and P brought about by the Shuram Excursion (Cui et al., 2016), to form calcium phosphate shells
- ❖ *Cloudina* transitioned to forming calcium carbonate shells later in the Ediacaran Period, due to the high availability of carbonate ions (Wood 2011; Wood et al., 2017) and decreased availability of P

❖ **Vital Effects: Hypothesis might be supported**

- ❖ It is possible that the recrystallized calcitic interior of the *Cloudina* were also drilled and included in the samples, so an alternative interpretation is that the *Cloudina* were cemented rapidly after death

❖ **Feeding Mechanism: More information is needed**

- ❖ Microbes that reduce sulfate tend to fractionate the S such that the resulting hydrogen sulfide (H_2S) is more enriched in ^{32}S (Kaplan & Rittenberg, 1964)
- ❖ H_2S may have been concentrated in *Cloudina* within a trophosome, contrary to the interpretation by Schiffbauer et al. (2020) that recently discovered internal cylindrical structures were a one-way through-gut
- ❖ Alternatively, H_2S may have been concentrated in the surficial microbial mat surrounding the *Cloudina*

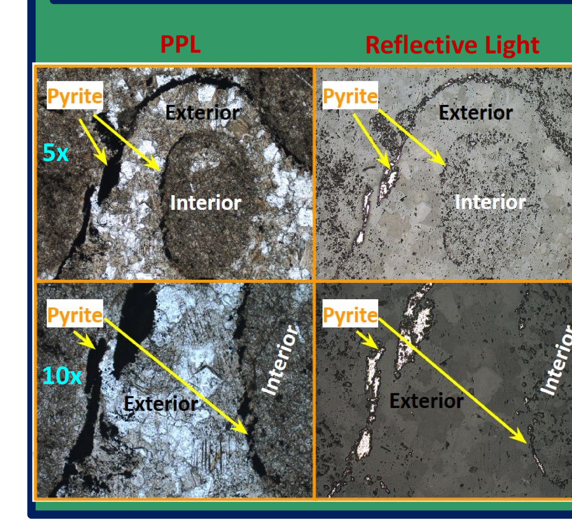

Figure 6: Suggestion for Future Work. Petrographic images of *Cloudina* from Spain show pyrite surrounding both the exterior and interior of *Cloudina*. Performing a secondary ion mass spectrometry (SIMS) analysis would allow for one to traverse across the *Cloudina* and measure the $\delta^{34}S$ values of the pyrite outside and inside the animal.

Acknowledgements & References

Special thanks go out to Dr. Jay Kaufman and Dr. Philip Piccoli for their advice throughout my senior thesis project. I would like to thank Julia Poggi and Orion Jenkins-Houk for their assistance with using Adobe Photoshop to outline and measure the orientation of *Cloudina*. I thank Dr. Piccoli for his assistance with the EPMA. I thank Dr. Penniston-Dorland for instructing me on how to use the petrographic microscope and rock saw. I am grateful to Dr. Steven Goderis and Dr. Huan Cui for providing data from the micro-XRF spectrometer. I thank Dr. Mike Evans, Dr. Jay Kaufman, Dr. Shuiwang Duan, and Cristy Ho for their assistance with the use of stable isotope mass spectrometers. I am grateful to Dr. Thomas Holtz for directing me to new published research on *Cloudina*. A final thanks goes out to the faculty that have given me constructive feedback on my presentations and proposal.

Becker-Kerber, B., Pacheco, M. L. A. F., Rudnitzki, I. D., Galante, D., Rodrigues, F., & Leme, J. M. (2017). Ecological interactions in Cloudina from the Ediacaran of Brazil: implications for the rise of animal biomineralization. *Sci. Rep., 7*(1), 1-11.

Cui, H., Xiao, S., Zhou, C., Peng, Y., Kaufman, A. J., & Plummer, R. E. (2016). Phosphogenesis associated with the Shuram Excursion: Petrographic and geochemical observations from the Ediacaran Doushantuo Formation of South China. *Sediment. Geol., 341*(2016), 134-146.

Felbeck, H. (1981). Chemoautotrophic Potential of the Hydrothermal Vent Tube Worm, Riftia pachyptila Jones (Vestimentifera). *Science*, *213*(4505), 336-338.

Fisher, C. R., Childress, J. J., & Minnich, E. (1989). Autotrophic Carbon Fixation by the Chemoautotrophic Symbionts of Riftia pachyptila. *Biol. Bull.*, *177*(3), 372-385.

Grant, S. W. F. (1992). Carbon isotopic vital effect and organic diagenesis, Lower Cambrian Forteau Formation, northwest Newfoundland: Implications for $\delta^{13}C$ chemostratigraphy. *Geology, 20*(3), 243-246.

Kaplan, I. R. & Rittenberg, S. C. (1964). Microbiological Fractionation of Sulfur Isotopes. *MicroSoc., 34*(2), 195-212.

Rooney, A. (2019). New Re-Os ages and Os geochemistry from the Neoproterozoic: Fresh insights into links between climate, animal evolution and biogeochemical cycles. *Geol. Soc. Am. Abstr., 51*(5).

Schiffbauer, J. D., Selly, T., Jacquet, S. M., Merz, R. A., Nelson, L. L., Strange, M. A., Cai, Y., & Smith, E. F. (2020). Discovery of bilaterian-type through-guts in cloudinomorphs from the terminal Ediacaran Period. *Nat. Commun., 11*(2020), 1-12.

Wood, R. (2011). Paleoecology of the earliest skeletal metazoan communities: Implications for early biomineralization. *Earth-Sci. Rev., 106*(1-2), 184-190.

Wood, R., Ivantsov, A. Y., & Zhuravlev, A. Y., Zhuravlev, A. Y. (2017). First macrobiota biomineralization was environmentally triggered. *Proc. Royal Soc. B, 284*(1851), 1-7.